PROCEEDINGS OF SPIE

SPIEDigitalLibrary.org/conference-proceedings-of-spie

The Maunakea Spectroscopic Explorer: throughput optimization

Nicolas Flagey, Shan Mignot, Kei Szeto, Alan McConnachie, Rick Murowinski

Nicolas Flagey, Shan Mignot, Kei Szeto, Alan McConnachie, Rick Murowinski, "The Maunakea Spectroscopic Explorer: throughput optimization," Proc. SPIE 9908, Ground-based and Airborne Instrumentation for Astronomy VI, 99089C (9 August 2016); doi: 10.1117/12.2231238

Event: SPIE Astronomical Telescopes + Instrumentation, 2016, Edinburgh, United Kingdom

Downloaded From: https://www.spiedigitallibrary.org/conference-proceedings-of-spie on 1/4/2018 Terms of Use: https://www.spiedigitallibrary.org/terms-of-use

The Maunakea Spectroscopic Explorer: throughput optimization

Nicolas Flagey[a], Shan Mignot[b], Kei Szeto[a], Alan McConnachie[a], and Rick Murowinski[a]

[a]Canada-France-Hawaii Telescope Corporation, 65-1238 Mamalahoa Hwy, Kamuela HI 96743, USA

[b]GEPI, Observatoire de Paris, PSL Research University, CNRS, Univ. Paris Diderot, Sorbonne Paris Cité, Place Jules Janssen, 92195 Meudon, FRANCE

ABSTRACT

The Maunakea Spectroscopic Explorer (MSE) will obtain millions of optical to near-infrared spectra, at low (R∼2,500) to high (R∼40,000) spectral resolution, via a highly multiplexed (∼3000) fiber-fed system. Key science programs for MSE (black hole reverberation mapping, stellar population analysis at high redshift, sub-km/s velocity accuracy for stellar astrophysics) will target faint Galactic and extra-galactic targets (typical visual magnitudes up to 24). MSE will thus need to achieve the highest throughput possible over the 360 to 1800 nm wavelength range. Here we discuss building an optimized throughput budget in terms of performance allocation and technical solutions to steer the concept design studies.

Keywords: throughput, fiber fed spectrograph

1. INTRODUCTION

The Maunakea Spectroscopic Explorer (MSE), previously known as the next generation Canada-France-Hawaii Telescope (ngCFHT), is a project to upgrade the 3.6-meter telescope and instrumentation of the CFHT into a 10-meter class telescope equipped with fiber-fed spectrographs dedicated to optical and near-infrared (NIR) spectroscopic surveys. The current baseline for MSE is that of a prime focus, 10-meter effective aperture telescope feeding a bank of low and moderate spectral resolution spectrographs (LMR, R∼2000-3500 and 6000) located on pseudo-Nasmyth platforms, as well as high spectral resolution spectrographs (HR, R∼20000 and 40000) located in the more stable environment of the telescope pier Coudé room. The 1.5 square degree field of view of MSE will be populated with more than 3200 fibers of about 1″ diameter allocated to the LMR spectrograph, and at least 1000 additional fibers for the HR spectrograph.

The ambition of MSE is to enable transformational science in the fields of tomographic mapping of the interstellar and intergalactic media, chemical tagging of the disk and halo stars, large scale structure, dark matter, reverberation mapping, and cosmological surveys. MSE will be the ultimate facility to study the composition and dynamics of the faint Universe. It will be the largest ground based optical telescope aside from the extremely large telescopes (E-ELT, TMT, GMT) and a critical follow-up observatory in the current and next generations of imaging surveys (LSST, Gaia, SKA, Euclid, WFIRST).

The status and progress of the project are detailed in Ref. 1 while an overview of the project design is given in Ref. 2, the science-based requirements are explained in Ref. 3, and details about the summit facility upgrade are presented in Ref. 4. Other papers at the 2016 SPIE meeting present optical designs for MSE,[5] a conceptual design of the High-Resolution Spectrograph,[6] systems budgets architecture and development,[7] observatory software,[8] and calibration challenges.[9]

The success of MSE will depend on its capability to obtain spectra of the faintest targets a ground telescope has ever reached with high multiplexing in the optical and near-infrared. To achieve this, the science requirements specify the system's sensitivity in terms of signal-to-noise ratios for the three resolution modes. The ambition is

Further author information: (Send correspondence to N.F.)
N.F.: E-mail: flagey@cfht.hawaii.edu

Ground-based and Airborne Instrumentation for Astronomy VI, edited by Christopher J. Evans, Luc Simard, Hideki Takami
Proc. of SPIE Vol. 9908, 99089C · © 2016 SPIE · CCC code: 0277-786X/16/$18 · doi: 10.1117/12.2231238

Downloaded From: https://www.spiedigitallibrary.org/conference-proceedings-of-spie on 1/4/2018 Terms of Use: https://www.spiedigitallibrary.org/terms-of-use

to allow the aforementioned observations to be sky-limited,[10] which implies that emphasis is placed on making the throughput of MSE as high as possible to increase the signal term.

In this paper we present the work we have done to carefully optimize the throughput and the necessary trade-offs that are necessary given the wide spectral range, the large field of view, the number of fibers. In addition, a balance has to be found between the ambitions of MSE and the minimization of the costs and risks inherent to novel techniques that require research and development. In section 2 we present the baseline parameters of MSE and the design choices that have already been made, which affect the overall throughput. In section 3, we describe the elements of the optical path and where we have opportunities for optimization. We then elaborate on the adopted strategies in Section 4, element by element. We conclude in section 5 with the overall throughput budget for MSE.

2. SCIENCE REQUIREMENTS

The Science Requirements Document defines the fundamental specifications that MSE shall meet. We briefly recall below those that have direct demands on the throughput optimization (others like radial velocity accuracy for example are omitted here). The challenge is to have MSE reach many very faint targets over a very broad wavelength range and a wide field of view, with a variety of spectral resolutions.

Spectral resolution: MSE will offer three resolution modes, from R∼2500–3000 in the Low Resolution (LR) mode, to R∼5000–7000 in the Moderate Resolution (MR) mode, and R∼20000 or 40000 (depending on the wavelength range) in the High Resolution (HR) mode.

Étendue: the effective étendue of MSE will be greater than 117 $m^2 deg^2$, with a field of view of at least 1 deg^2 that can be tiled in a regular pattern.

Multiplexing: in LR and MR mode, at least 3200 objects will be observed simultaneously, while in HR mode, the spectra of at least 1000 objects will be obtained.

Spectral coverage: MSE will cover the entire optical range at wavelengths longer than 360 nm and up to 950 nm at all resolutions, as well as the J and H bands in LR mode only. The spectral range observed at once in MR mode will be at least 250 nm wide, and that in HR mode will be comprised of 2 or 3 individual windows about 20 nm wide.

Sensitivity: in LR mode, MSE will obtain a signal-to-noise ratio (SNR) of at least 2 per resolution element for a target with an AB magnitude of 24, in 1 hour, at all wavelengths larger than 400 nm, with a natural seeing of $0.8''$ in r band, an airmass of 1.2, and a sky brightness of 20.7 mag/arcsec^2 in V band. In MR mode, the same will be true for a target with an AB magnitude of 23.5 instead. In HR mode, the SNR will be greater than 10 for a target with an AB magnitude of 20 and a sky brightness of 19.5 mag/arcsec^2 in V band.

3. OVERVIEW OF OPTICAL TRAIN

The baseline design of MSE is shown in Figure 1. Details about the upgrade of the summit building and about the telescope design are given in Refs. 2 and 4. Here we describe the optical train and the design choices that impact on throughput optimization and have already been made.

Enclosure: the dome will be a calotte, similar to that of the Thirty Meter Telescope, rather than a slit. The dome will have vents to maintain image quality, similar to those installed on CFHT's dome.[11]

Telescope structure: open-truss to facilitate ventilation and mirror flushing.

Downloaded From: https://www.spiedigitallibrary.org/conference-proceedings-of-spie on 1/4/2018 Terms of Use: https://www.spiedigitallibrary.org/terms-of-use

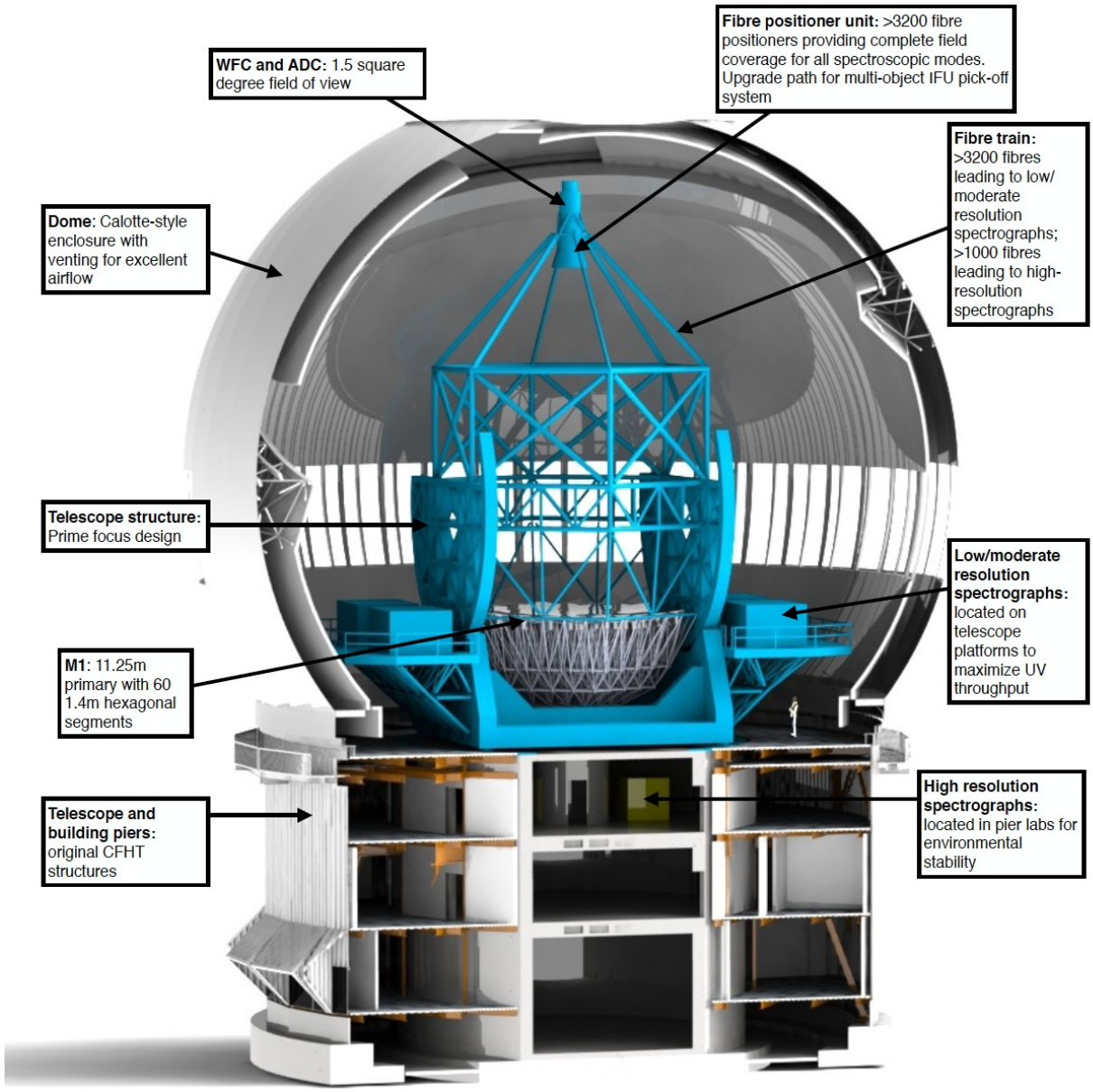

Figure 1. Overview of the baseline design for MSE.

Downloaded From: https://www.spiedigitallibrary.org/conference-proceedings-of-spie on 1/4/2018 Terms of Use: https://www.spiedigitallibrary.org/terms-of-use

Table 1. Wavelengths chosen for the throughput optimization.

Wavelength	Rationale
360 370 400	sampling of the extreme blue coverage
445	center of B band
551	center of V band
658	center of R band
900	center of Z band
1000	extremity of the optical passband
1114 1220 1327	extremities and center of J band
1477 1630 1784	extremities and center of H band

Optical design: MSE will be a Prime Focus telescope on an Alt-Az mount. The primary mirror will comprise 60 hexagonal segments of 1.44 m (central segment removed). A Prime Focus Upper End (PFUE) will consist of a Wide Field Corrector (WFC), an Atmospheric Distortion Correction (ADC), the fiber positioners, the instrument rotator, and the acquisition and guiding system. The PFUE is mounted on a hexapod system which compensates for gravity and temperature effects.

Multi-object spectroscopy: MSE will be fiber fed. The fiber positioners will be either of the Echidna or Phi-Theta type. There will be two different sets of fibers for the HR spectrographs and the LMR spectrographs. The number of positioners that will carry two fibers will depend, primarily, on the type of positioner selected after conceptual design reviews.

Spectrographs: the LR and MR modes will be provided by the same spectrographs. These LMR spectrographs will be located on platforms while the HR spectrographs will be located further away in the stable environment of the telescope pier Coudé room.

The main parameters under considerations for throughput optimization are as follows:

- the reflective coating of the primary mirror,
- the anti-reflection coating of the lenses in the PFUE, their number, their dimensions,
- the type of fiber positioners, the diameter of the fibers, and the length of the fiber train,
- the number of arms in the spectrograph, their central wavelengths and widths.

This paper discusses MSE's throughput optimization from the perspective of the science requirements and technical decisions hitherto made. The discussion happens in the context of, e.g. a broad wavelength coverage imposed by the Science Requirements (360 to 1800 nm, with an emphasis on wavelengths longer than 400 nm) which results in the need for high performance broad band coatings, and the image quality of the site and the facility which is needed to maximize the injection of targets' photons into the fibers. To assess performance in a scientifically and technically meaningful way, reference wavelengths have been defined over the complete wavelength range and are presented in Table 1.

4. THROUGHPUT ELEMENTS

In this section we discuss throughput performance of the various elements in the optical train, from the atmosphere to the detectors in the spectrographs.

Downloaded From: https://www.spiedigitallibrary.org/conference-proceedings-of-spie on 1/4/2018 Terms of Use: https://www.spiedigitallibrary.org/terms-of-use

4.1 Atmosphere

While not technically part of the system, a critical decision to be made is about the location of the observatory: MSE will be built at the top of the best site for astronomy in the Northern hemisphere.

There are several sites on the planet that are known for the quality of their astronomical skies: Maunakea, the Chilean Andes, the Canary Islands, Antarctica, San Pedro Mártir. These sites have been selected to install observatories because of their clearer and dryer atmosphere, their darker sky, the number of clear nights per year and the sharpness of the images they deliver. The recent site testing studies by the Thirty Meter Telescope project has shown that summits in Chile and Maunakea were the best sites for optical/infrared ground astronomy.[12] The site of CFHT, on the Eastern ridge of Maunakea, has been considered the best within the astronomy precinct due to the smooth ascend of the site from sea level that minimizes ground level turbulence.

For MSE's sensitivity, the dark sky means lower background (i.e. less noise) and the clear nights mean increased observing efficiency (i.e. higher photon collection per year). The exquisite seeing is important for injecting as much of the targets' light into the fibers even with a reduced diameter, especially given the "flat" sky background contribution that increases with the size of the fibers. Last but not least, the altitude of the observatory (CFHT is installed at an altitude of 4200 m) means that the attenuation by the atmosphere is reduced.

4.2 Primary mirror

The primary mirror of MSE will be 11.25 m in diameter, making it the largest optical/near-infrared telescope in the world after the extremely large telescopes (TMT, GMT, E-ELT). The mirror is comprised of 60 hexagonal segments of 1.44 m, arranged in a honeycomb pattern, similar to the Keck telescopes, with no central segment. The effective aperture for the unvignetted 60 segments (80.8m^2) will be that of a 10.14 m circular aperture telescope, hereafter used as the zero-loss aperture reference.

Given the science requirements on sensitivity, the goal for MSE is to obtain the best throughput from 360 nm to 1800 nm, with a focus on wavelengths larger than 400 nm. The Gemini telescopes use a protected silver coating that provides a good baseline for the primary mirror of MSE. Silver coating provides an increased reflectivity compared to aluminum, except at wavelengths shorter than about 480 nm. Figure 2 shows the reflectivity for Gemini's primary mirror silver coating and that for aluminum coating, along with other coating performance curves. Over the 360 to 1800 nm range, the average silver and aluminum reflectivity are 96.4 and 93.9%, respectively. Averaged over the 400 to 1800 nm range, the silver performance rises slightly to 96.7% while that of the aluminum remains unchanged.

Also shown on Figure 2 are the requirements and goals for the Thirty Meter Telescope, which aims at covering a much broader spectral range than MSE, from very blue to mid-infrared. However, to our knowledge, the coating for TMT is still under development. The Gemini Observatories, through careful maintenance, have maintained very high efficiency of their mirror coating.[13] Besides, it is possible to improve on these results by protecting the coating from light and dust when the telescope is not in operation. Progress and new techniques for protected silver coatings have been studied at University of California Observatories Advanced Coatings Lab and it has been shown that a reflectivity higher than 96% at all wavelengths between 340 and 1200 nm can be achieved.[14] Field testing however revealed significant degradation of the coating when exposed to observatory environment. Performances advertised by CILAS, for instance, for classical protected silver and UV-enhanced silver coatings are also shown in the Figure 2. They correspond to an average reflectivity of 95.0 and 96.4%, respectively, between 360 and 1800 nm, which increase to 95.6 and 96.7%, respectively, between 400 and 1800 nm.

The goal for MSE is to achieve better performances than Gemini at very short wavelengths, while maintaining a high reflectivity throughout, though without requiring the same bandpass as TMT. We also aim at recoating the 60 segments of the primary mirror through the course of two years, thanks to a rolling mechanism and a number of spare segments, thus allowing the overall reflectivity to decrease only by about 1% annually. To limit the demand on operations (complexity and cost) with the need to recoat 1 segment about every 2 weeks, a simple recoating process is favored, e.g. limit multiple layers, prefer deposition via evaporation rather than sputtering. Both aluminum and protected silver coatings thus remain possible options at this stage of the project, though the silver coating offers better performances in the wavelength range of interest for MSE, i.e. wavelengths longer than 400 nm.

Downloaded From: https://www.spiedigitallibrary.org/conference-proceedings-of-spie on 1/4/2018 Terms of Use: https://www.spiedigitallibrary.org/terms-of-use

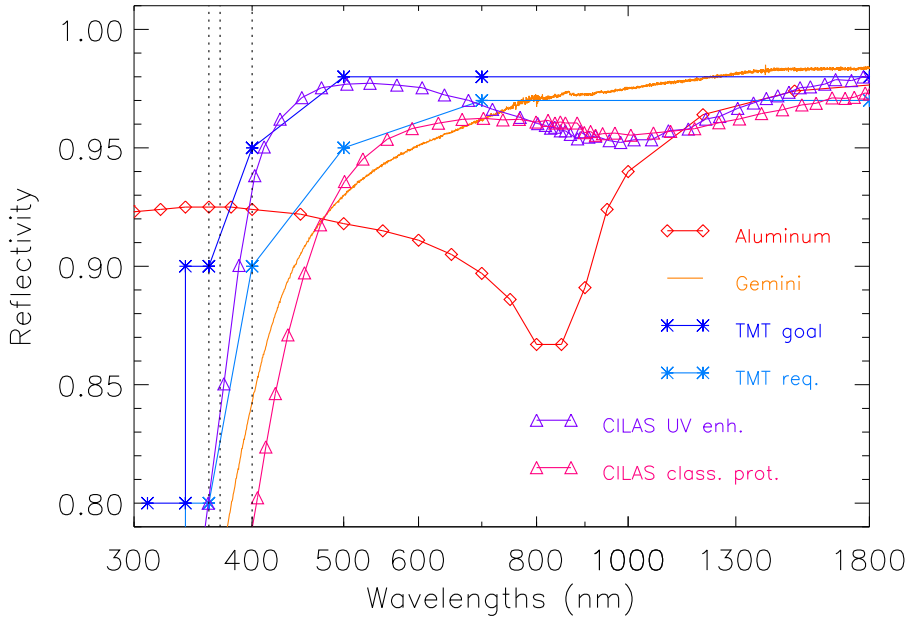

Figure 2. Reflectivity of Gemini's primary mirror (solid orange) compared to the requirements and goals for TMT (blue stars). The performance achieved by UV-enhanced and classical protected silver coatings by CILAS (purple and pink triangles), and aluminum coating (red diamonds) are also given for comparison.

4.3 Enclosure and telescope structure

The opening on the calotte will be 12.5 m wide to allow telescope on-sky tracking without continuous motion of the enclosure. Making the opening bigger would be challenging for the structure of the cap and the enclosure. It is assumed and requested that the enclosure will not vignette the beam during observations and that during exposures that require motion of the dome, the enclosure will not affect performances of the observatory (e.g. vibrations).

The top end spider, which supports the prime focus upper end (PFUE), necessarily intersects the beam. With the current design of the telescope structure,[2] the vignetting from the spider does not exceed 3% which is consistent with the 2% allocated in our budget. Care shall be taken, however, to ensure that no telescope structural members lead to increased vignetting the edge of the primary mirror. The fiber bundles which carry the photons from the PFUE to the spectrographs, together with the various data links and utilities (electricity, coolant, etc.), must be located in the "shadow" of the spider legs and will not contribute to additional vignetting.

4.4 Prime Focus Upper End

The PFUE consists of several systems: the hexapod, the WFC and ADC opto-mechanics, the instrument rotator, the fiber positioners, and the optical feedback system for pointing, guiding, and image quality monitoring.

Given the length of the telescope and its aperture, the optimal size of the first lens in the WFC/ADC can only be within a range that will not significantly obscure the central part of the primary mirror or limit the field of view of the telescope, given the available fused silica blank size. The central segment of the primary mirror, which is not installed, corresponds to a 1.26 m inscribed circle. Therefore, as soon as the diameter of the whole PFUE (including the lens barrel and baffle) becomes larger than 1.26 m, there will be central obscuration. The current baseline is to have a first lens 1.3 m in diameter, which corresponds to 4% vignetting loss for the WFC/ADC design.[5] The size of the other four lenses are scaled according to this diameter. The whole PFUE is thus about 1.75 m in diameter and contributes to an additional 1% loss via central obscuration. The technical limitations on the size of blanks are reached at about this diameter for PBM2Y too.

Downloaded From: https://www.spiedigitallibrary.org/conference-proceedings-of-spie on 1/4/2018 Terms of Use: https://www.spiedigitallibrary.org/terms-of-use

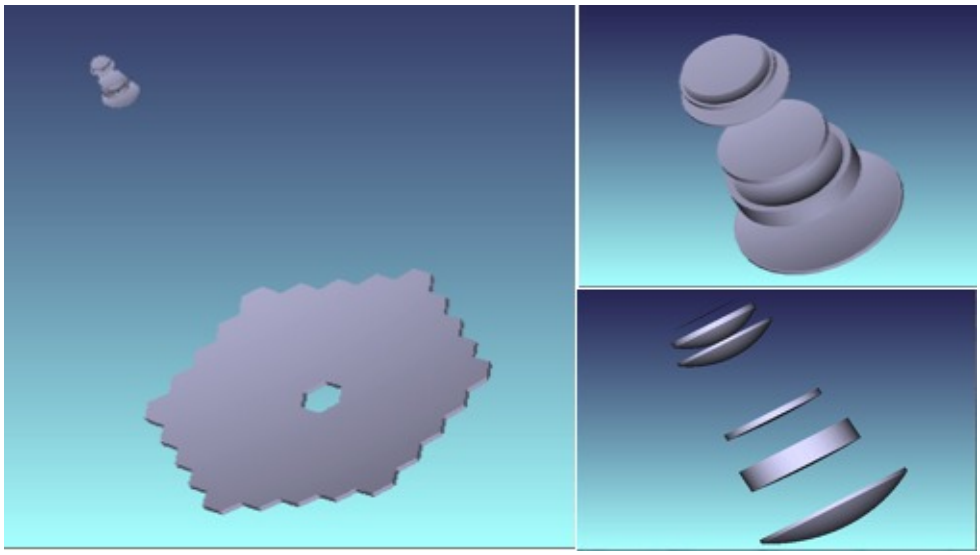

Figure 3. Proposed optical design for the PFUE.

The WFC consists of a group of lenses that removes off-axis low-order aberrations and the ADC compensates the dispersion induced by the variation of the air's refractive index with wavelength, which naturally increases with zenith distance due to airmass. Given MSE's large wavelength range, the number of lenses in the optical design, the glass types used and the AR coating characteristics are important parameters which affect the throughput. The current design of the WFC/ADC comprises 5 lenses. Based on Ref. 15, the usual ADC doublet is removed and its function achieved by moving one of the WFC's lenses laterally while the whole WFC moves in the other direction. As a result 3 lenses are of fused silica which has very good transmission over the MSE bandwidth and only 2 are PBM2Y to correct for chromatic aberrations at a small expense on throughput. The large optics thickness of the WFC still cause measurable throughput losses. As an example, for a lens 210 mm thick, absorption ranges from <1% (synthetic fused-silica) to 6% (BSL7Y) at 1µm. Our budget is set at 1% loss per lens on average here.

With multi-layer anti-reflection coatings, Fresnel losses (i.e. reflection) can be minimized. Attempting to cover the 360 nm to 1.8 µm range is challenging however. The performance of the multi-layer coatings degrade as function of wavelength range. In addition, a trade-off needs to be made between maximum mid-range performance with poor behavior on the edges (up to 5%) or more balanced overall profiles. Performances per surface up to 0.1% in the visible but degrading smoothly down to between 1% and 2% in the UV and NIR have been reported.[5] A conservative approach of an average 1% per surface was adopted here between 360 and 1000 nm and 2% between 1000 and 1800 nm. Sol-gel over MgF2 is an alternative with potentially better performances but its technical readiness level is low for large optics like those envisioned for MSE.

To limit the number of optical surfaces, we choose to avoid using an optical derotator to correct for field rotation and prefer a mechanical solution instead, under the assumption that the mechanics of the field rotator, prescribed in the PFUE barrel, shall not vignette the beam coming from the WFC/ADC.

Putting all the contributors together, we therefore budget a 5% throughput loss for the PFUE, with 4% due to vignetting and 1% to central obscuration, and transmission efficiencies of at least 86% up to 1000 nm and at least 78% at longer wavelengths. Overall, the entire PFUE shall have a throughput of at least 82% up to 1000 nm and 74% beyond.

4.5 Fiber train

The focal plane of MSE will be populated with thousands of fibers: at least 3200 allocated to the LMR spectrographs, and at least 1000 to the HR spectrographs. Whether the positioners are of the Echidna or Phi-Theta type, the fiber train can be optimized in several ways. We first discuss the injection at the focal plane and then the transmission along the fiber train.

Downloaded From: https://www.spiedigitallibrary.org/conference-proceedings-of-spie on 1/4/2018 Terms of Use: https://www.spiedigitallibrary.org/terms-of-use

The fiber characteristic that may have the most effect on the throughput is the injection near the focal surface. The fraction of energy that enters the fiber, at any wavelength, is the critical metric for throughput. The injection efficiency relies on a complex analysis that includes: image quality, fiber positioning and tracking, atmospheric refraction, chromatic effects, and fiber diameter. Ideally, each fiber should be perfectly centered on its target in the focal surface from the beginning to the end of the integration, while the image quality and the fiber diameter should match to allow as much flux as possible to go through the fiber. Our analysis shows that for a target on axis and at zenith, a positioning error of the order of 10 µm (the combined positioning accuracy which includes positioner, pointing, tracking, star catalog astrometry, ...) will lead to losses of about 2%, while tilting the fiber by 1.5° corresponds a 5% loss. For a target away from zenith and off-axis, these losses increase up to 18% and 22% due to chromatic and angular effects. While improving the efficiency might call for increasing the fiber core, it would lead to higher noise due to an increase in sky background contribution. As a result the optimized sizes for the fibers result from a trade-off analysis which takes the targets characteristics and sky magnitudes into account, and likely lead to HR fibers of different core diameter than the LMR fibers. The budget currently assumes a 70% injection efficiency at wavelengths shorter than 400 nm and 75% otherwise.

The transmission along the fibers is affected by focal ratio degradation losses, Fresnel losses and the lengths of the fibers. Stress and macro-bending causing FRD (independent of potential losses due to vignetting at the collimator level in the spectrographs) and misalignment of fibers versus the chief rays are estimated based on the ngCFHT Telescope optical design. Since FRD is weakly dependent on fiber length,[16] a common value is adopted here for LMR and HR fibers. FRD losses resulting from twisting the fibers is neglected here as tests for the development of the MOONS fiber system have shown that in spite of significant twisting (up to 7 per meter), the 1% loss in flux proved smaller than the fiber-to-fiber performance variations (4%).[17]

Some AR coating will be required to reduce Fresnel losses at the input and output of the fibers. We here assume micro-lenses on input and plane windows on output (gluing with an optical gel is preferable than polishing the fiber). For the HR fibers, the spectral coverage is sufficiently limited and the variation of indices can be effectively limited thanks to the optical gel and only the very first and last surfaces have a significant impact (with optimized AR coating). For the LMR fibers however, this does not seem to be the case and three surfaces have to be considered for the micro-lens and window respectively.

High numerical aperture fibers ($NA \sim 0.3$) would present some advantages as they would not require micro-lenses at the injection into the fibers. Therefore, throughput would increase thanks to the reduction of the number of optical surfaces, the removal of the potential alignment issue between fiber and micro-lens, and the absence of gluing process. The overall system would also be simplified without the need to attach thousands of micro-lenses to the fibers.

Optical fibers have good transmission characteristics in the visible domain but they degrade very quickly in the UV. Therefore the LMR spectrographs, which have the most stringent requirement in terms of throughput (i.e. sensitivity), shall be placed closer to the telescope. A trade-off then needs to be made between throughput and instrument stability. Placing the spectrographs on the telescope has proven impractical because of the varying impact of gravity. More effectively, pseudo-Nasmyth platforms provide a shorter fiber distance, although the spectrographs are submitted to varying environmental conditions in the dome, such as temperature, vibrations, and wind.

The length of the fibers should be minimized to limit the losses. However, the design of the telescope structure, the location of the spectrographs, the vignetting of the beam by the fiber bundles, and the need to limit stress/torsion/flexure of the fiber, leave room for optimization. Considering the telescope structure length from the PFUE to the LMR spectrographs platforms (about 20 to 25 meters, see Figure 4) and the need to incorporate stress relieving mechanisms (2–3 meters),[18] LMR fibers are expected to be 30 m long at most. Twist in the LMR fibers will only result from movement of the telescope in altitude, and most of the twist will occur somewhere near the elevation axis. The HR fibers need to follow a similar path down to the elevation axis, but then reach the Coudé room. This will add about 15 to 20 meters, relative to the LMR fibers, for a total length of about 45 to 50 m. The HR fibers will be subjected to additional twist due to the telescope motion in azimuth. The twist will be limited to about 270° in both directions and will occur mostly within the pier. We assume the fiber throughput will be similar to those of Polymicros FBP or FBPI fibers. No connector will be used along the

Downloaded From: https://www.spiedigitallibrary.org/conference-proceedings-of-spie on 1/4/2018 Terms of Use: https://www.spiedigitallibrary.org/terms-of-use

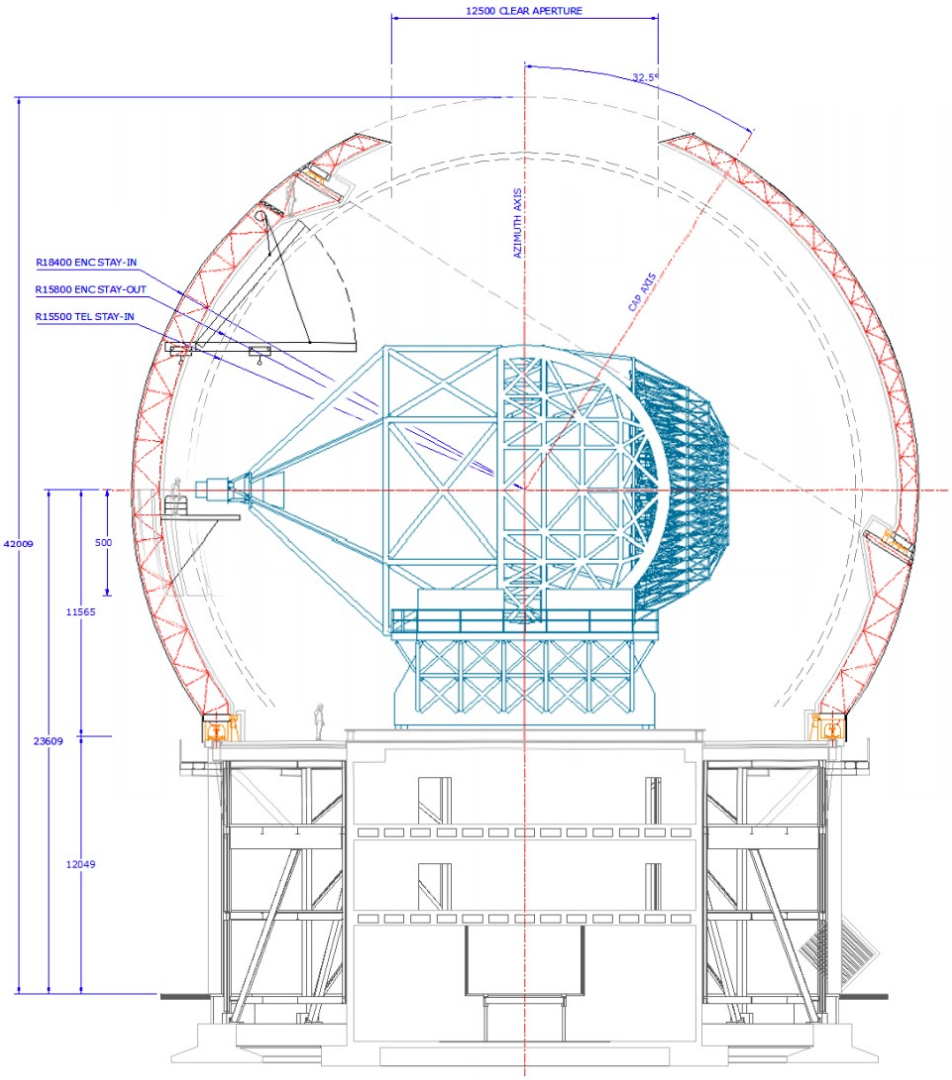

Figure 4. Proposed design for the enclosure and telescope structure.

Downloaded From: https://www.spiedigitallibrary.org/conference-proceedings-of-spie on 1/4/2018 Terms of Use: https://www.spiedigitallibrary.org/terms-of-use

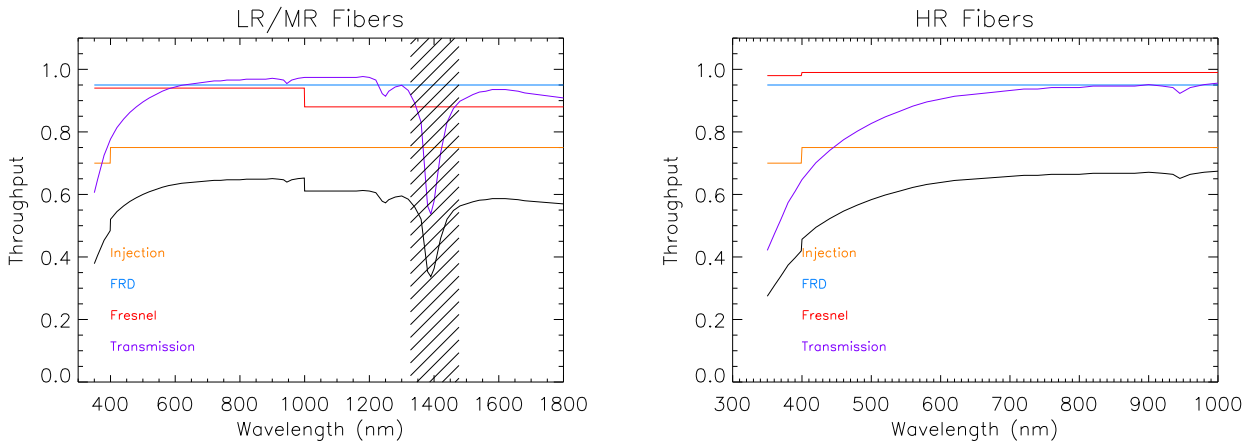

Figure 5. Throughput requirement for the fibers. The hatched area corresponds to the atmospheric band of absorption between J and H bands. The LMR fibers are 30 m long, while the HR fibers are 50 m long.

fiber transmission system to maintain throughput. The overall budget for the fibers throughput is indicated in Figure 5.

4.6 Spectrographs

The conceptual design for the HR spectrograph is presented in Ref. 6. The main design challenges are related to the wavelength windows that need to be observed simultaneously, their widths, and the frequency at which these windows will be modified. Additionally, large aperture telescopes usually are at a disadvantage when it comes to high spectral resolution, as it requires larger optics in the spectrograph, higher dispersion elements, and a reduced slit size with the addition of slicers. All of these design considerations come at a cost, in terms of throughput and in terms of complexity and size (i.e. price) of the HR spectrographs.

For the LMR spectrographs, the main challenges are meeting the requirements on sensitivity and spectrophotometry. Even more challenging than reaching the largest throughput possible, the spectrophotometry requirement implies an accurate knowledge of the throughput during the observations for all the fibers in the field of view. With MSE, we shall be able to measure and calibrate how the throughput varies with pointing, telescope field position, fiber, environmental conditions, and field position. This involves an accurate understanding of the derivatives of the throughput as a function of all these parameters. More details about a design solution currently envisaged for MSE can be found in Ref.[19]

Hereafter, we describe the performances that are budgeted for the various assemblies of both the LMR and HR spectrographs, assuming a simple though realistic design. Figure 6 shows a schematic concept for the spectrographs, with four arms, Volume Phase Holographic Gratings (VPHGs) as dispersive elements, and Schmidt cameras. For the MR and HR spectrographs, additional elements are necessary (prisms, image slicers).

4.6.1 FRD losses

The faster f-ratio of the output beam due to FRD in the fibers may cause a loss in throughput if the beam becomes wider than the collimator's mirror. Since FRD is a random effect which varies from fiber to fiber, and given the configuration of the fiber train (geometry, stress), setting a threshold to FRD losses implies over-sizing the collimator to match the statistical distribution of f-ratios. In our budget, we assume that the FRD at the collimator level shall cause throughput losses lower than 1% averaged over all fibers.

4.6.2 Input misalignment

A misalignment between the pseudo-slit and the collimator will cause a loss in throughput because of angular deviation and/or lateral displacement. Misalignment is usually of very limited impact since the collimator must be designed to accommodate the field corresponding to the slit length and uses optics with circular symmetry. Therefore, the collimator is largely over-sized compared to the fibers' far-field, parallel and perpendicular to the

Downloaded From: https://www.spiedigitallibrary.org/conference-proceedings-of-spie on 1/4/2018 Terms of Use: https://www.spiedigitallibrary.org/terms-of-use

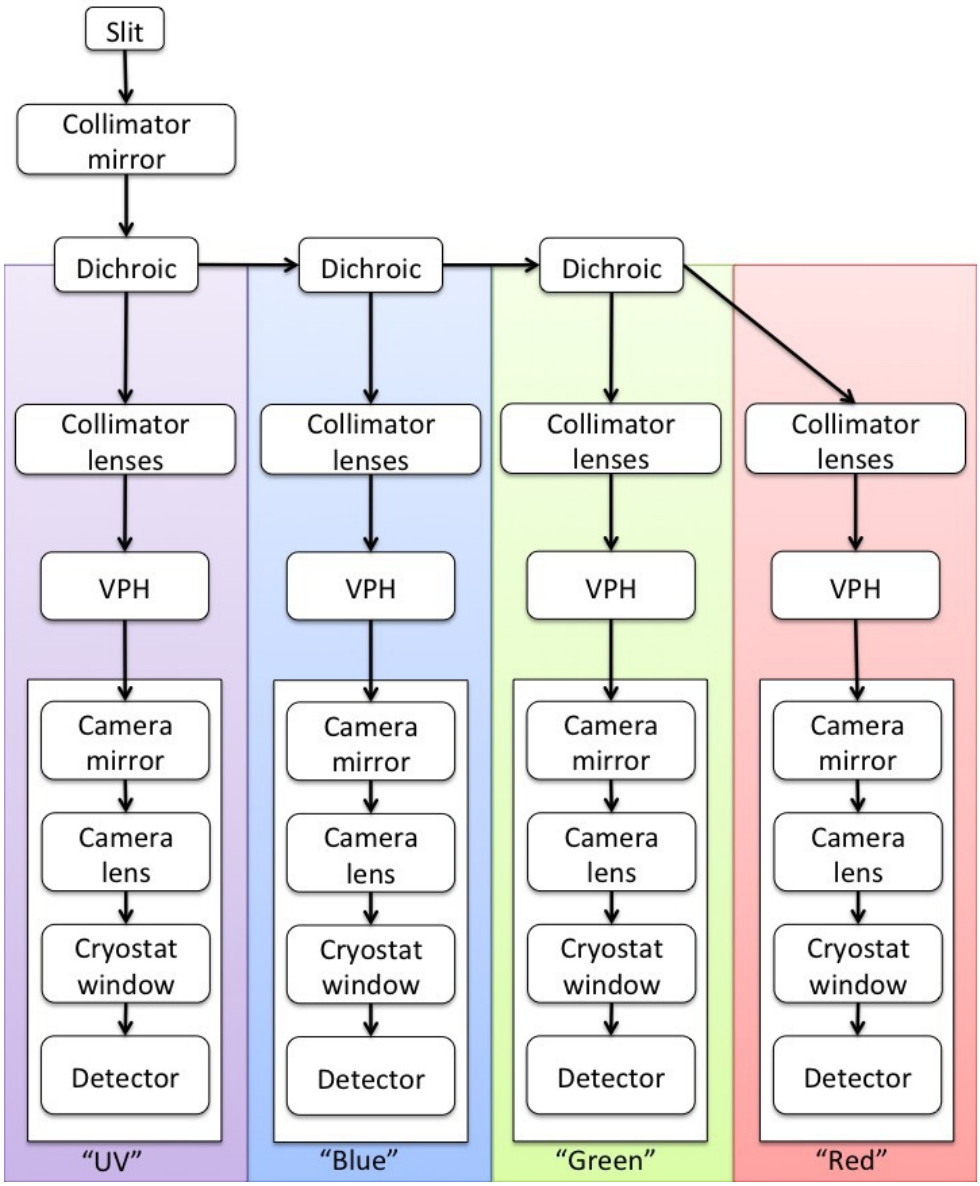

Figure 6. Block diagram of the optical path in the strawman concept for the LR spectrograph. In the MR case, 2 prisms should be added before and after each VPH to form a grism. In the HR case, an image slicer composed of two mirrors should be added after the collimator lenses.

Downloaded From: https://www.spiedigitallibrary.org/conference-proceedings-of-spie on 1/4/2018 Terms of Use: https://www.spiedigitallibrary.org/terms-of-use

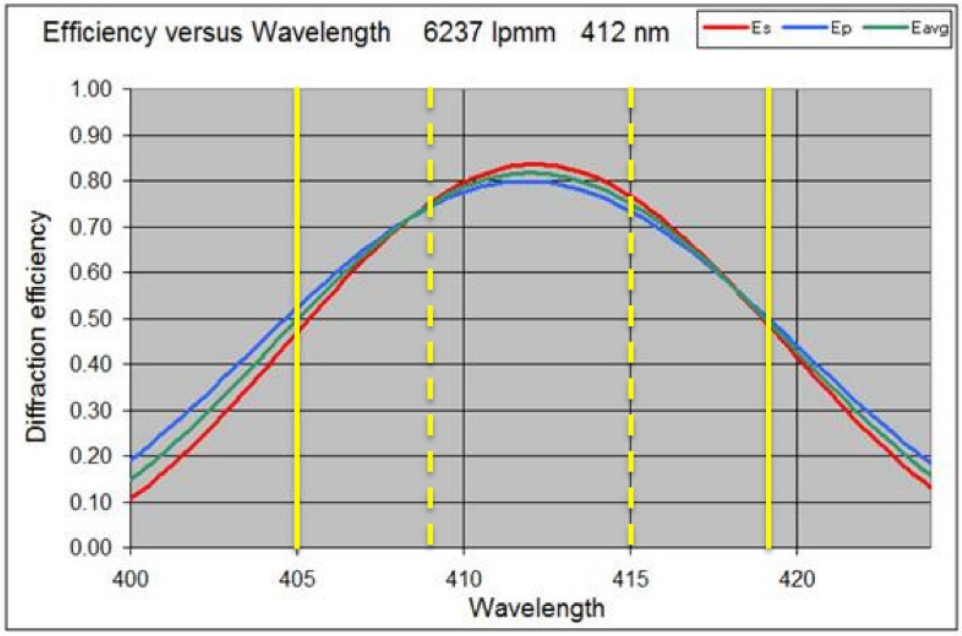

Figure 7. Diffraction efficiency of a high groove density (6237 lines per mm, 58 degrees Bragg angle) VPHG at 412 nm designed for high dispersion of the HR spectrograph.

slit direction. The only fibers likely to be substantially affected by alignment losses are located at the extremities of the slit since their far-field is projected near the edge of the collimator mirror. A conservative 1% estimate of losses is hence adopted here.

4.6.3 Dispersive optics

The dispersion in the spectrographs is the second bottleneck in the overall throughput budget with the injection in the fibers at the focal surface.

VPHGs are the components with the highest efficiency on the market with maxima potentially above 90%. However, their efficiency curve is bell-like and their performance drops quickly (see Figure 7), which could be problematic for the HR spectrographs. The exact profile depends on the dispersion required: the greater the number of lines per millimeter and the greater the value of the optimum angle of incidence (Bragg angle), the lower the maximum efficiency and the faster the decrease. In the example shown, the efficiency reaches slightly more than 80% at 412 nm, and stays above 50% for only about 14 nm, with 6237 lines per mm, a Bragg angle of 58 degree, and a prism in S-BSL7. The current baseline for the HR spectrograph is described in details in Ref.6.

In our throughput performance allocation, we budget an efficiency of the VPHG exceeding 70% over all of the spectral coverage of MSE to preserve performance. As illustrated in Figure 7, this is not readily achieved for wide wavelength bands. A potential work-around is to split the wavelength ranges that need to be observed in as many intervals as necessary so that each VPHG only works at its maximum efficiency. Such a requirement has strong cost and complexity implications since the number of arms in the spectrographs, each with their VPHG and camera, may become significant although their individual design will be simplified due to the smaller wavelength coverage leading to smaller focal planes.

4.6.4 Other optics

The other optics to consider in the spectrograph designs are:

- collimator: one mirror (silver-coated) and two corrector lenses – these are assumed to be after the dichroics so their AR coatings can be optimized for each arm of the spectrograph,

Downloaded From: https://www.spiedigitallibrary.org/conference-proceedings-of-spie on 1/4/2018 Terms of Use: https://www.spiedigitallibrary.org/terms-of-use

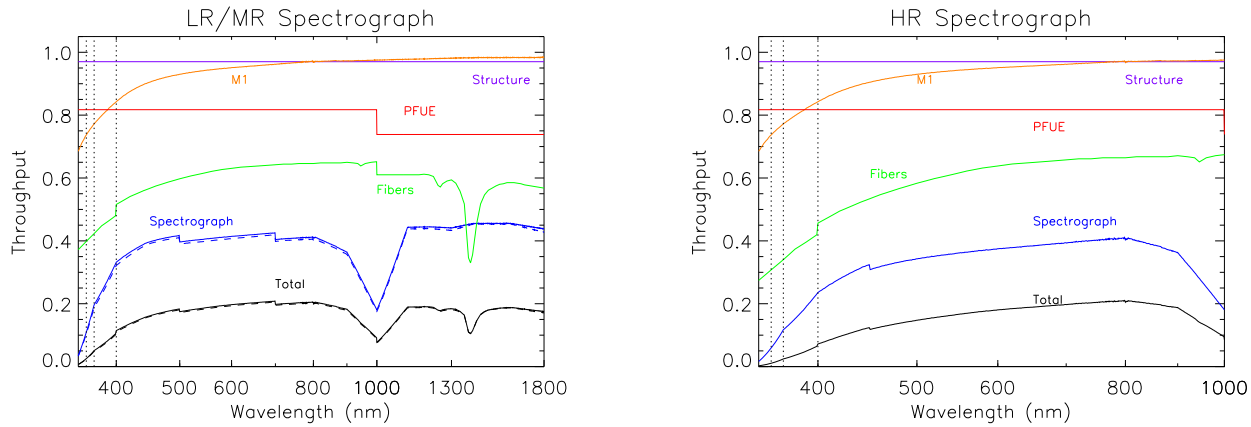

Figure 8. Overall expected throughput (without the atmosphere) for MSE with the contribution of each subsystem highlighted. *Left:* LMR spectrograph (medium resolution is the dashed-line). *Right:* HR spectrograph.

- dichroics: arranged serially to split the collimated spectrograph beam into three arms, whose division are assumed to be at 450 and 600 nm for the HR spectrographs, and at 500, 700, and 1000 nm for the LMR spectrographs, with the J and H band sharing an arm,
- two glass plates for each VPH,
- one window for each of the cryostats, with optimized AR coating,
- 2 prisms are added before and after each VPH to form a grism in the MR spectrographs,
- an image slicer composed of two mirrors is added before the collimator lenses in the HR spectrographs,
- Schmidt cameras: they image the spectra at fast f-ratios to avoid oversampling of the spectra and reduce the cost dependence on the size of the beams. They use one silver-coated mirror, one lens with optimized AR coating, and the central obstruction by the detector is assumed to be 15%.

4.6.5 Detectors

The detectors in the spectrographs will be CCDs for the visible part of the spectrum and CMOS for the near-infrared. Candidate choices for the optical are e2v detectors, with peak quantum efficiency at 90% between 400 nm and 800 nm, or Hamamatsu detectors, such as those recently developed for the Hyper Suprime-Cam project, which perform well up to 1000 nm.[20,21] For the near-infrared detectors, the choice is rather limited: Teledyne Hawaii-2RG and 4RG are potential candidates. The cut-off between the visible and infra-red detectors will be set to minimize cost and maximize quantum efficiency over the whole wavelength range. Here we assume the cut-off will be at 1000 nm.

5. CONCLUSION

Figure 8 shows the overall budgeted throughput for MSE and the contributions from different elements in the optical path. In both LMR and HR spectrographs, the performances are currently budgeted to provide a throughput as uniform as possible at wavelengths longer than 400 nm with additional access to the wavelengths down to 360 nm, and correspond to the baselines for the LMR and HR spectrograph designs currently being developed.[6,19]

The optimization of the baseline will evolve with the refinement of the science case and in particular the prioritization of the observations as a function of wavelengths, sensitivity, and spectral resolution. In addition, several trade-offs are still being investigated, especially the access to very short wavelengths, the exact cut-off wavelength between visible and infrared ranges, and the modularity of the infrared arm.

Downloaded From: https://www.spiedigitallibrary.org/conference-proceedings-of-spie on 1/4/2018 Terms of Use: https://www.spiedigitallibrary.org/terms-of-use

Table 2. Throughput, in percent, for each instrument and each major element in the optical train.

Wavelength (nm)	Telescope structure	Primary mirror	PFUE	Fibers		Spectrograph			**Total**		
				LMR	HR	LR	MR	HR	**LR**	**MR**	**HR**
360	97	73	81	39	30	10	10	5	**2**	**2**	**1**
370	97	77	81	42	34	19	18	11	**5**	**4**	**2**
400	97	84	81	51	45	33	32	23	**11**	**11**	**7**
445	97	90	81	56	52	39	38	31	**15**	**15**	**12**
551	97	94	81	61	61	40	39	36	**18**	**18**	**16**
658	97	95	81	63	65	42	41	38	**20**	**20**	**19**
806	97	97	81	64	66	41	40	40	**20**	**20**	**20**
900	97	97	81	64	67	36	35	36	**18**	**17**	**18**
1000	97	97	73	61	67	18	17	18	**7**	**7**	**8**
1114	97	97	73	61	67	44	43	-	**18**	**18**	**-**
1220	97	97	73	60	66	44	43	-	**18**	**18**	**-**
1327	97	98	73	57	60	44	43	-	**17**	**17**	**-**
1477	97	98	73	55	58	45	45	-	**17**	**17**	**-**
1630	97	98	73	58	62	45	44	-	**18**	**18**	**-**
1784	97	98	73	56	60	43	42	-	**17**	**17**	**-**

REFERENCES

[1] Murowinski, R., McConnachie, A. W., Simons, D., and Szeto, K., "Maunakea Spectroscopic Explorer: the status and progress of a major site redevelopment project," in [*Ground-based and Airborne Telescopes VI*], *Proc. SPIE* **9906** (July 2016).

[2] Szeto, K., Bai, H., Bauman, S., Crampton, D., Flagey, N., Fouque, P., Gillingham, P., Gong, X., Ho, K., McConnachie, A., Mignot, S., Murowinski, R., Salmon, D., Spano, P., Zhai, C., and Zhang, K., "Maunakea Spectroscopic Explorer design development from feasibility concept to baseline design," in [*Ground-based and Airborne Telescopes VI*], *Proc. SPIE* **9906** (July 2016).

[3] McConnachie, A. W., "Science-based requirement and operations development for the Maunakea Spectroscopic Explorer," in [*Ground-based and Airborne Telescopes VI*], *Proc. SPIE* **9906** (July 2016).

[4] Bauman, S. E., Green, G., and Szeto, K., "Maunakea Spectroscopic Explorer observatory upgrade: a revised and optimized astronomical facility," in [*Ground-based and Airborne Telescopes VI*], *Proc. SPIE* **9906** (July 2016).

[5] Saunders, W. and Gillingham, P. R., "Optical designs for the Maunakea Spectroscopic Explorer telescope," in [*Ground-based and Airborne Telescopes VI*], *Proc. SPIE* **9906** (July 2016).

[6] Zhang, K., Zhu, Y., and Hu, Z., "Maunakea Spectroscopic Explorer: conceptual design of multiobject high resolution spectrograph," in [*Ground-based and Airborne Instrumentation for Astronomy VI*], *Proc. SPIE* **9908** (July 2016).

[7] Mignot, S. B., Flagey, N., Szeto, K., Murowinski, R., and McConnachie, A. W., "Systems budgets architecture and development for the Maunakea Spectroscopic Explorer," in [*Modeling, Systems Engineering, and Project Management for Astronomy VI*], *Proc. SPIE* **9911** (July 2016).

[8] Vermeulen, T. A., Isani, S., Withington, K. K., Ho, K. K. Y., Szeto, K., and Murowinski, R., "Observatory software for the Maunakea Spectroscopic Explorer," in [*Software and Cyberinfrastructure for Astronomy IV*], *Proc. SPIE* **9913** (July 2016).

[9] Flagey, N., McConnachie, A. W., Murowinski, R., Szeto, K., and Mignot, S. B., "Spectral calibration for the Maunakea Spectroscopic Explorer: challenges and solutions," in [*Observatory Operations: Strategies, Processes, and Systems VI*], *Proc. SPIE* **9910** (July 2016).

[10] Flagey, N., Mignot, S. B., Szeto, K., McConnachie, A. W., and Murowinski, R., "The Maunakea Spectroscopic Explorer: throughput optimization," in [*Ground-based and Airborne Instrumentation for Astronomy VI*], *Proc. SPIE* **9908** (July 2016).

Downloaded From: https://www.spiedigitallibrary.org/conference-proceedings-of-spie on 1/4/2018 Terms of Use: https://www.spiedigitallibrary.org/terms-of-use

[11] Bauman, S. E., Benedict, T., Baril, M., Culiandre, J. C., Look, I., Matsushige, G., Roberts, L., Racine, R., Salmon, D., and Vermeulen, T., "Dome venting: the path to thermal balance and superior image quality," in [*Observatory Operations: Strategies, Processes, and Systems V*], *Proc. SPIE* **9149**, 91491K (Aug. 2014).

[12] Schöck, M., Els, S., Riddle, R., Skidmore, W., Travouillon, T., Blum, R., Bustos, E., Chanan, G., Djorgovski, S. G., Gillett, P., Gregory, B., Nelson, J., Otárola, A., Seguel, J., Vasquez, J., Walker, A., Walker, D., and Wang, L., "Thirty Meter Telescope Site Testing I: Overview," *PASP* **121**, 384–395 (Apr. 2009).

[13] Vucina, T., Boccas, M., Araya, C., and Ahhee, C., "Gemini's protected silver coatings: first two years in operation," in [*Society of Photo-Optical Instrumentation Engineers (SPIE) Conference Series*], *Proc. SPIE* **6273**, 62730W (June 2006).

[14] Phillips, A. C., Fryauf, D. M., Kobayashi, N. P., Bolte, M. J., Dupraw, B., Ratliff, C., Pfister, T., and Cowley, D., "Progress and new techniques for protected-silver coatings," in [*Advances in Optical and Mechanical Technologies for Telescopes and Instrumentation*], *Proc. SPIE* **9151**, 91511B (July 2014).

[15] Saunders, W., Gillingham, P., Smith, G., Kent, S., and Doel, P., "Prime focus wide-field corrector designs with lossless atmospheric dispersion correction," in [*Advances in Optical and Mechanical Technologies for Telescopes and Instrumentation*], *Proc. SPIE* **9151**, 91511M (July 2014).

[16] Pazder, J., Fournier, P., Pawluczyk, R., and van Kooten, M., "The FRD and transmission of the 270-m GRACES optical fiber link and a high numerical aperture fiber for astronomy," in [*Advances in Optical and Mechanical Technologies for Telescopes and Instrumentation*], *Proc. SPIE* **9151**, 915124 (July 2014).

[17] Guinouard, I., Lee, D., Schnetler, H., Taylor, W., Amans, J.-P., Montgomery, D., and Oliva, E., "Development of the fibres of MOONS," in [*Advances in Optical and Mechanical Technologies for Telescopes and Instrumentation*], *Proc. SPIE* **9151**, 91514S (July 2014).

[18] de Oliveira, A. C., de Oliveira, L. S., de Arruda, M. V., Souza Marrara, L., dos Santos, L. H., Ferreira, D., dos Santos, J. B., Rosa, J. A., Junior, O. V., Pereira, J. M., Castilho, B., Gneiding, C., Junior, L. S., de Oliveira, C. M., Gunn, J., Ueda, A., Takato, N., Shimono, A., Sugai, H., Karoji, H., Kimura, M., Tamura, N., Wang, S.-Y., Murray, G., Le Mignant, D., Madec, F., Jaquet, M., Vives, S., Fisher, C., Braun, D., Schwochert, M., and Reiley, D. J., "Fiber optical cable and connector system (FOCCoS) for PFS/ Subaru," in [*Advances in Optical and Mechanical Technologies for Telescopes and Instrumentation*], *Proc. SPIE* **9151**, 91514G (July 2014).

[19] Saunders, W., "Very fast transmissive spectrograph designs for highly multiplexed fiber spectroscopy ," in [*Ground-based and Airborne Instrumentation for Astronomy VI*], *Proc. SPIE* **9908** (July 2016).

[20] Kamata, Y., Miyazaki, S., Nakaya, H., Suzuki, H., Miyazaki, Y., and Muramatsu, M., "Characterization and performance of hyper Suprime-Cam CCD," in [*High Energy, Optical, and Infrared Detectors for Astronomy IV*], *Proc. SPIE* **7742**, 774229 (July 2010).

[21] Miyazaki, S., Komiyama, Y., Nakaya, H., Kamata, Y., Doi, Y., Hamana, T., Karoji, H., Furusawa, H., Kawanomoto, S., Morokuma, T., Ishizuka, Y., Nariai, K., Tanaka, Y., Uraguchi, F., Utsumi, Y., Obuchi, Y., Okura, Y., Oguri, M., Takata, T., Tomono, D., Kurakami, T., Namikawa, K., Usuda, T., Yamanoi, H., Terai, T., Uekiyo, H., Yamada, Y., Koike, M., Aihara, H., Fujimori, Y., Mineo, S., Miyatake, H., Yasuda, N., Nishizawa, J., Saito, T., Tanaka, M., Uchida, T., Katayama, N., Wang, S.-Y., Chen, H.-Y., Lupton, R., Loomis, C., Bickerton, S., Price, P., Gunn, J., Suzuki, H., Miyazaki, Y., Muramatsu, M., Yamamoto, K., Endo, M., Ezaki, Y., Itoh, N., Miwa, Y., Yokota, H., Matsuda, T., Ebinuma, R., and Takeshi, K., "Hyper Suprime-Cam," in [*Ground-based and Airborne Instrumentation for Astronomy IV*], *Proc. SPIE* **8446**, 84460Z (Sept. 2012).

Downloaded From: https://www.spiedigitallibrary.org/conference-proceedings-of-spie on 1/4/2018 Terms of Use: https://www.spiedigitallibrary.org/terms-of-use